ResearchGate

See discussions, stats, and author profiles for this publication at: https://www.researchgate.net/publication/263947837

Vapor–Liquid Equilibrium, Densities, and Interfacial Tensions of the System Hexane + 2,5-Dimethylfuran

ARTICLE *in* JOURNAL OF CHEMICAL & ENGINEERING DATA · SEPTEMBER 2012

Impact Factor: 2.04 · DOI: 10.1021/je300631s

CITATIONS
6

READS
43

4 AUTHORS:

Andres Mejia
University of Concepción
82 PUBLICATIONS **618** CITATIONS
SEE PROFILE

Hugo Segura
University of Concepción
146 PUBLICATIONS **1,287** CITATIONS
SEE PROFILE

Marcela Cartes
University of Concepción
30 PUBLICATIONS **167** CITATIONS
SEE PROFILE

Joao A. P. Coutinho
University of Aveiro
483 PUBLICATIONS **12,337** CITATIONS
SEE PROFILE

Available from: Joao A. P. Coutinho
Retrieved on: 04 February 2016

Journal of chemical & engineering data

Article

pubs.acs.org/jced

Vapor−Liquid Equilibrium, Densities, and Interfacial Tensions of the System Hexane + 2,5-Dimethylfuran

Andrés Mejía,*[,†] Hugo Segura,*[,†] Marcela Cartes,[†] and João A. P. Coutinho[‡]

[†]Departamento de Ingeniería Química, Universidad de Concepción, POB 160-C, Correo 3, Concepción, Chile

[‡]Departamento de Química, CICECO, Universidade de Aveiro, Campus Universitário de Santiago, 3810-193 Aveiro, Portugal

ABSTRACT: Vapor−liquid equilibrium (VLE) data at isobaric conditions (50, 75, and 94) kPa and over the temperature range (331 to 364) K have been measured for the binary system hexane + 2,5-dimethylfuran using a dynamic VLE cell. Mixture densities were also determined at 298.15 K and atmospheric pressure with a vibrating tube densimeter, whereas atmospheric interfacial tension of the mixture was measured at 303.15 K using a maximum differential bubble pressure tensiometer. Because few experimental data are available; pure component vapor pressures, densities, and interfacial tensions have also been measured for 2,5-dimethylfuran over the temperature range (293 to 367) K. According to the reported experimental results, the entitled zeotropic mixture exhibits positive deviation from ideal behavior. The mixing volumes in turn, are positive over the whole mole fraction range. Finally, it is also experimentally observed that the interfacial tensions exhibit negative deviation from the linear behavior. The reported VLE data of the binary mixture are thermodynamically consistent according to Fredenlund's test and were well-correlated by classic activity coefficients (Wohl, nonrandom two-liquid, Wilson) and by the universal quasi-chemical model for all of the measured isobars. The Redlich−Kister equation was used to correlate the mixing volumes as well as interfacial tensions.

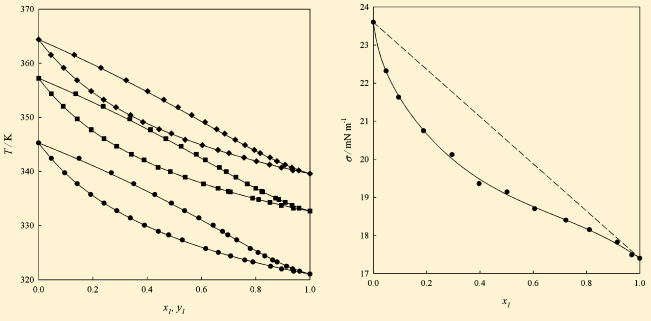

INTRODUCTION

Since 1990, the Clean Air Act Amendments have been pressing oil companies to reduce air and ground harmful emissions by adding oxygen-rich compounds to transportation fuels. Due to their technical and economical feasibility, branched ethers (such as 2-methoxy-2-methylbutane or TAME, 2-methoxy-2-methylpropane or MTBE, 2,2′-oxybis[propane] or DIPE, and 2-ethoxy-2-methyl-propane or ETBE) and linear alcohols (e.g., methanol, ethanol, butanol) have been considered as typical commercial additives. However, present facts and constraints such as feedstock supplies, environmental regulations, and economic issues have been forcing fuel producers and researchers to search not only for new oxygenated additives but also for alternative fuels (such as biofuels)[1] able to reduce the environmental impact from automotive transportation.

A promising new fuel additive is 2,5-dimethylfuran (or DMF) which, reportedly, has been found to exhibit attractive technical and commercial characteristics. For example, from a process production viewpoint, Román-Leshkov et al.[2] have proposed a novel and high yield biochemical route able to efficiently produce DMF from sugar. According to Román-Leshkov et al., DMF can be obtained from fructose through a catalytic biomass-to-liquid process. The main advantage of the proposed biochemical synthesis is the raw material: fructose, which can be obtained from fruit and some root vegetables or, alternatively, from glucose, which can be derived from either starch or cellulose. As a potential new fuel, DMF exhibits an energy density similar to that of gasoline and superior to, by approximately 40%, that of ethanol.[3]

The Research Octane Number (RON) of DMF is 119, which is comparable to the gasoline RON (95.8) and ethanol RON (110).[2] The high DMF RON would allow its use in high compression ratio engines, thus resulting in improved fuel economy.[4] Another important feature of DMF is its stoichiometric air/fuel ratio of 10.72, which is lower than the stoichiometric air/fuel ratio of gasoline (14.56). This lower ratio implies that burning of DMF requires 35% less air than gasoline. As a clear proof of its applicability, DMF has been successfully tested as a fuel in a direct-injection spark-ignition engine, showing an excellent performance.[5] Finally, among its attributes, it has been verified that (a) DMF is chemically stable, (b) DMF is immiscible with water and unable to absorb moisture from the atmosphere, and (c) its evaporation requires approximately one-third less energy than the evaporation of ethanol. On the basis of the quoted characteristics and on additional findings of recent reports,[2,5−8] DMF clearly qualifies as new potential and highly efficient biofuel.

To rationally explore applications of DMF in gasoline blending and as biofuel, it is required to complement customary mechanical tests with an appropriate thermo-physical characterization. Particularly, vapor−liquid equilibrium (VLE) data provide

Received: May 3, 2012
Accepted: August 27, 2012
Published: September 6, 2012

 © 2012 American Chemical Society dx.doi.org/10.1021/je300631s | J. Chem. Eng. Data 2012, 57, 2681−2688

Table 1. Reported Purities (Mass Fraction), Refractive Index n_D at the Na D Line at Temperature T = 298.15 K, Densities ρ at Temperature T = 293.15 K, Normal Boiling Points T_b at Pressure p = 101.33 kPa, and Interfacial Tensions σ at Temperature T = 303.15 K of Pure Components[a]

	n_D		ρ / g·cm^{-3}		T_b / K		σ / mN·m^{-1}	
component (purity/mass fraction)	exp	lit.	exp	lit.	exp	lit.	exp	lit.
hexane (0.99)	1.37374	1.37230[b]	0.659776	0.66050[b]	341.94	341.88[b]	17.40	17.37[b]
DMF (0.99)	1.44040	c	0.90118	0.90300[d]	366.83	366.15[e]	24.04	c

[a]Standard uncertainties u are $u(n_D) = \pm 10^{-5}$, $u(\rho) = 5\cdot10^{-6}$ g·cm^{-3}, $u(T_b) = \pm 0.02$ K, $u(\sigma) = \pm 0.2$ mN·m^{-1}, $u(T) = \pm 0.01$ K, $u(p) = \pm 0.03$ kPa. [b]Daubert and Danner.[11] [c]Not available value. [d]Verevkin and Welle.[9] [e]Alvarez et al.[13]

Table 2. Experimental Mass Densities ρ and Interfacial Tensions σ as a Function of Temperature T for DMF[a]

T / K	ρ / g·cm^{-3}	σ / mN·m^{-1}
293.15	0.90118	25.42
303.15	0.89037	24.04
313.15	0.87943	22.73
323.15	0.86836	21.41
333.15	0.85710	20.22
343.15	0.84567	19.10
353.15	0.83401	18.05
358.15	0.82813	17.50

[a]Standard uncertainties u are $u(T) = \pm 0.01$ K, $u(\rho) = 5\cdot10^{-6}$ g·cm^{-3}, and $u(\sigma) = \pm 0.2$ mN·m^{-1}.

Table 3. Experimental Vapor Pressures p as a Function of Temperature T for DMF[a]

T / K	p / kPa
331.46	30.01
335.51	35.01
339.09	40.01
342.32	45.01
345.26	50.01
348.00	55.01
350.53	60.01
352.90	65.01
355.13	70.01
357.24	75.01
359.24	80.01
361.13	85.01
362.95	90.01
364.69	95.01
366.79	101.33

[a]Standard uncertainties u are $u(T) = \pm 0.02$ K, $u(p) = \pm 0.03$ kPa.

useful information for characterizing the distillation curve (fuel concentration during vaporization) and the Reid vapor pressures (volatility indicator) for possible gasoline blending applications. Density data, or V^E, are needed for designing appropriate engine injection systems and optimal vessels for fuel transportation and storage. IFT data, in turn, are needed to characterize the formation and ignition kinetics of fuel drops. To the best of our knowledge, the available experimental data for DMF are scarce and limited to pure fluid vapor pressures[9] and densities.[9,10] For the case DMF based mixtures, neither VLE, mixing volumes (or V^E), nor IFT data have been previously reported. Consequently, this work is undertaken to measure new

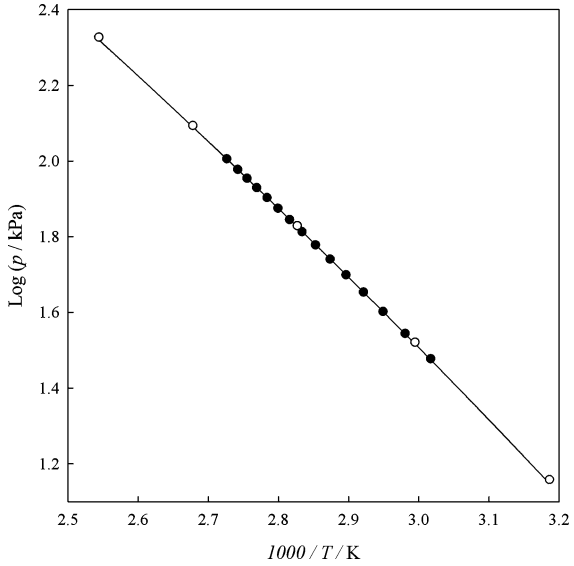

Figure 1. Vapor pressure (p) as a function of temperature (T) for pure DMF. —, predicted by eq 2. Experimental reported data: ●, this work; ○, Zaitri et al.[22]

experimental data of vapor−liquid equilibrium (VLE), densities (and excess volumes, V), and interfacial tensions (IFT) of pure DMF and of the hexane + DMF binary mixture.

EXPERIMENTAL SECTION

Chemicals. Hexane and 2,5-dimethylfuran were purchased from Merck and Aldrich, respectively, and they were used without further purification. Table 1 reports the purity of the components declared by Merck and Aldrich, respectively. A gas chromatography (GC) test confirms a mass purity not less than indicated by the companies. Table 1 also includes the refractive indexes (n_D) at 298.15 K, the liquid mass densities (ρ) at 293.15 K, the normal boiling points (T_b), and the interfacial tensions (σ) of pure fluids at 303.15 K. Table 1 also includes the corresponding reference values reported in the literature[9,11−13] for the measured pure fluid properties.

Apparatus and Procedure. Vapor−liquid equilibrium (VLE) data were measured by using an all-glass VLE Fischer cell model 601 (Fischer Labor and Verfahrenstechnik). In this VLE cell, the temperature accuracy was ± 0.02 K whereas the pressure was measured with an estimated accuracy of ± 0.03 kPa. Densities were measured using an Anton Paar DMA 5000 vibrating U-tube densitymeter, with an accuracy of $5\cdot10^{-6}$ g·cm^{-3} and the temperature of the densitymeter was kept constant to within ± 0.01 K. The refractive indexes were measured using a Multiscale Automatic Refractometer RFM 81 (Bellingham + Stanley) with an uncertainty of ± 10^{-5} and

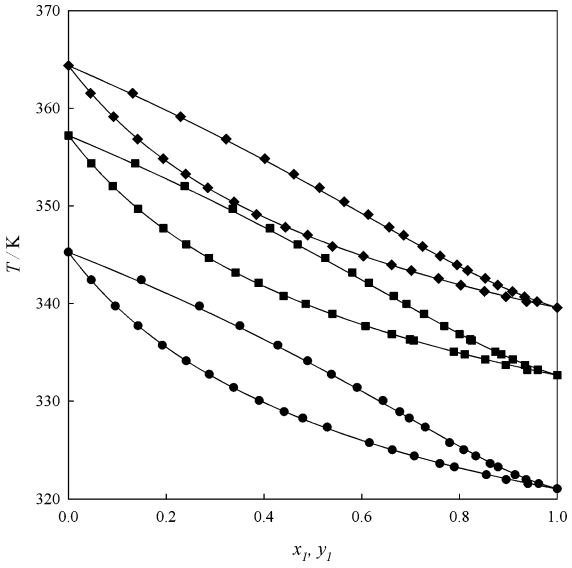

Figure 2. Isobaric phase diagram for the system hexane (1) + DMF (2). Experimental data at: ●, 50.00 kPa; ■, 75.00 kPa; ◆, 94.00 kPa; —, predicted from the two-parameter Legendre polynomial used in consistency analysis (Table 7).

Table 4. Experimental VLE Data for Temperature T, Pressure p = 50.00 kPa, Liquid-Phase Mole Fraction x, Vapor-Phase Mole Fraction y, for the Binary System Hexane (1) + DMF (2)[a,b]

T					$-B_{ij}$ / cm^3·mol^{-1}		
K	x_1	y_1	γ_1	γ_2	ij = 11	ij = 22	ij = 12
345.24	0.000	0.000		1.000		1340	
342.40	0.047	0.149	1.581	0.987	1309	1370	1333
339.73	0.096	0.268	1.512	0.984	1335	1399	1361
337.71	0.142	0.351	1.419	0.991	1356	1422	1382
335.71	0.192	0.428	1.366	0.997	1377	1445	1404
334.11	0.241	0.489	1.310	1.007	1394	1464	1422
332.73	0.288	0.538	1.259	1.024	1409	1480	1438
331.38	0.338	0.591	1.230	1.028	1424	1497	1453
330.04	0.390	0.644	1.214	1.024	1439	1513	1469
328.89	0.441	0.678	1.174	1.057	1452	1527	1482
328.23	0.479	0.697	1.137	1.094	1460	1536	1490
327.31	0.530	0.730	1.111	1.120	1470	1548	1501
325.72	0.616	0.780	1.077	1.192	1489	1568	1521
325.00	0.663	0.809	1.063	1.215	1498	1578	1530
324.36	0.708	0.834	1.049	1.254	1505	1586	1538
323.60	0.760	0.863	1.038	1.296	1515	1596	1548
323.26	0.790	0.879	1.030	1.324	1519	1601	1552
322.46	0.855	0.914	1.016	1.417	1529	1612	1562
321.97	0.896	0.937	1.012	1.479	1535	1619	1569
321.55	0.940	0.963	1.005	1.557	1540	1624	1574
321.03	1.000	1.000	1.000		1546		

[a]Standard uncertainties u are $u(T)$ = ± 0.02 K, $u(p)$ = ± 0.03 kPa, and $u(x_1) = u(y_1)$ = ± 0.01. [b]γ_i is the activity coefficient of component i, and B_{ij} is the molar virial coefficient.

the temperature was maintained constant to within ± 0.01 K. Interfacial tensions were measured using a PC500-LV Sensadyne maximum differential bubble pressure tensiometer with an accuracy of ± 0.2 mN·m^{-1}. In tensiometric measurements, the temperature of the sample was maintained constant

Table 5. Experimental VLE Data for Temperature T, Pressure p = 75.00 kPa, Liquid-Phase Mole Fraction x, Vapor-Phase Mole Fraction y, for the Binary System Hexane (1) + DMF (2)[a,b]

T					$-B_{ij}$ / cm^3·mol^{-1}		
K	x_1	y_1	γ_1	γ_2	ij = 11	ij = 22	ij = 12
357.21	0.000	0.000		1.000		1225	
354.35	0.047	0.137	1.532	0.991	1199	1251	1219
352.01	0.091	0.238	1.467	0.990	1220	1273	1241
349.69	0.142	0.336	1.418	0.986	1240	1296	1262
347.71	0.194	0.413	1.345	0.993	1258	1315	1281
346.06	0.241	0.469	1.291	1.009	1274	1332	1297
344.66	0.288	0.525	1.264	1.007	1287	1346	1311
343.16	0.342	0.581	1.229	1.014	1301	1362	1326
342.12	0.389	0.615	1.180	1.041	1312	1373	1336
340.75	0.440	0.666	1.176	1.036	1325	1388	1350
339.96	0.485	0.692	1.134	1.069	1333	1397	1358
338.93	0.540	0.727	1.106	1.098	1344	1408	1369
337.68	0.608	0.769	1.080	1.142	1356	1422	1383
336.84	0.662	0.800	1.059	1.182	1365	1432	1392
336.30	0.699	0.822	1.049	1.204	1371	1438	1398
336.20	0.707	0.826	1.045	1.216	1372	1439	1399
335.07	0.789	0.873	1.025	1.280	1384	1452	1411
334.79	0.811	0.886	1.020	1.306	1387	1456	1414
334.25	0.853	0.909	1.013	1.358	1393	1462	1420
333.69	0.895	0.934	1.010	1.404	1399	1469	1427
333.21	0.939	0.960	1.005	1.484	1404	1474	1432
332.65	1.000	1.000	1.000		1410		

[a]Standard uncertainties u are $u(T)$ = ± 0.02 K, $u(p)$ = ± 0.03 kPa, and $u(x_1) = u(y_1)$ = ± 0.01. [b]γ_i is the activity coefficient of component i, and B_{ij} is the molar virial coefficient.

to within ± 0.01 K using a Julabo thermostatic bath. Liquid and vapor-phase mole fractions were determined by gas chromatography (GC) using a thermal conductivity detector. Column, injector, and detector temperatures in GC were (373.15, 383.15, and 493.15 K) respectively; conditions in which concentration measurement accuracies were better than ± 0.01 in mole fraction. More specific details concerning experimental procedures can be found in ref 14 and in recent reports of our group.[15−19]

It is important to establish that although density measurements provide an accurate alternative for determining equilibrium-phase mole fractions, a large sample volume is usually required. Consequently, in VLE determinations, the GC technique was preferred to (a) reduce equilibrium perturbations during phase sampling by means of the use of negligible sample volumes and (b) avoid preferential vaporization of components during the manipulation of samples

■ RESULTS AND DISCUSSION

Pure Fluids. Reliable thermophysical properties for hexane such as density, vapor pressure, and interfacial tension have been extensively reported (see refs 20 and 21). Table 1 summarizes some reference values for the properties of the quoted components, whereas eq 1 correlates hexane's vapor pressure (P_i^0) over the temperature (T) from 307.66 to 342.08 K:[18]

$$\log(P_i^0/\mathrm{kPa}) = 6.02073 - 1182.8673/[(T/\mathrm{K}) - 47.3254] \quad (1)$$

dx.doi.org/10.1021/je300631s | J. Chem. Eng. Data 2012, 57, 2681−2688

Table 6. Experimental VLE Data for Temperature T, Pressure p = 94.00 kPa, Liquid-Phase Mole Fraction x, Vapor-Phase Mole Fraction y, for the Binary System Hexane (1) + DMF (2)[a,b]

T					$-B_{ij}$ / cm^3·mol^{-1}		
K	x_1	y_1	γ_1	γ_2	ij = 11	ij = 22	ij = 12
364.37	0.000	0.000		1.000		1162	
361.54	0.045	0.131	1.568	0.990	1140	1186	1158
359.14	0.092	0.229	1.434	0.993	1159	1207	1178
356.83	0.142	0.323	1.396	0.992	1178	1228	1198
354.81	0.194	0.402	1.339	0.994	1195	1247	1215
353.25	0.240	0.462	1.297	0.998	1209	1261	1229
351.86	0.285	0.514	1.261	1.003	1221	1274	1242
350.40	0.339	0.565	1.215	1.018	1234	1289	1255
349.11	0.385	0.614	1.205	1.014	1246	1301	1268
347.80	0.444	0.656	1.160	1.043	1258	1314	1280
346.99	0.489	0.686	1.126	1.066	1265	1323	1288
345.84	0.540	0.725	1.115	1.077	1276	1334	1299
344.84	0.604	0.760	1.077	1.127	1285	1345	1309
343.96	0.661	0.795	1.055	1.163	1294	1354	1318
343.36	0.701	0.817	1.040	1.203	1300	1360	1324
342.57	0.757	0.853	1.029	1.224	1307	1369	1332
341.87	0.803	0.878	1.021	1.274	1314	1376	1339
341.23	0.852	0.908	1.014	1.307	1320	1383	1345
340.69	0.895	0.933	1.008	1.372	1326	1389	1351
340.17	0.937	0.959	1.004	1.444	1331	1395	1356
339.57	1.000	1.000	1.000		1337		

[a]Standard uncertainties u are $u(T) = \pm 0.02$ K, $u(p) = \pm 0.03$ kPa, and $u(x_1) = u(y_1) = \pm 0.01$. [b]$\gamma_i$ is the activity coefficient of component i, and B_{ij} is the molar virial coefficient.

Available experimental properties are quite scarce for the case of DMF. In fact, only a few density[9,10] measurements and vapor pressure data[9] are available. Consequently, this work undertakes some basic measurements of the properties of pure DMF, which are required later in data treatment section. Particularly, Table 2 reports new density (ρ) and interfacial tension (σ) measurements as a function of temperature, where it is seen that both ρ and σ decrease with temperature, as expected. In addition, Table 3 reports experimental values of the vapor pressure as a function of temperature, which have been measured using the same VLE still described before. The vapor pressure data P_i^0 were smoothed using the Antoine equation:

$$\log(P_i^0/\text{kPa}) = 5.64673 - 1011.4342/[(T/\text{K}) - 89.0388] \quad (2)$$

The vapor pressure data of DMF are adequately described by eq 2 with an average absolute percentage deviation (AAPD) of 0.13 %. Figure 1 exhibits a comparison between the vapor pressure predicted from eq 2 with the experimental data reported by Zaitri et al.[22] Inside its temperature range, eq 2 predicts the data reported in ref 22 with an average deviation of $\delta P/P$ = 0.87 %. In addition, from Figure 1, we can observe a good agreement between the present vapor pressure data and that reported Zaitri et al.[22]

Isobaric Vapor−Liquid Equilibrium. Figure 2 illustrates the phase equilibrium behavior of hexane + 2,5-dimethylfuran binary mixture and Tables 4 to 6 report the numerical values of the experimental equilibrium temperature T, liquid x_i, and vapor-phase y_i mole fractions of component i at the three isothermal conditions (50, 75, and 94) kPa considered in this work.

Tables 4 to 6 and Figures 3 to 5 also report the activity coefficients (γ_i) that have been calculated according to the expression:[23]

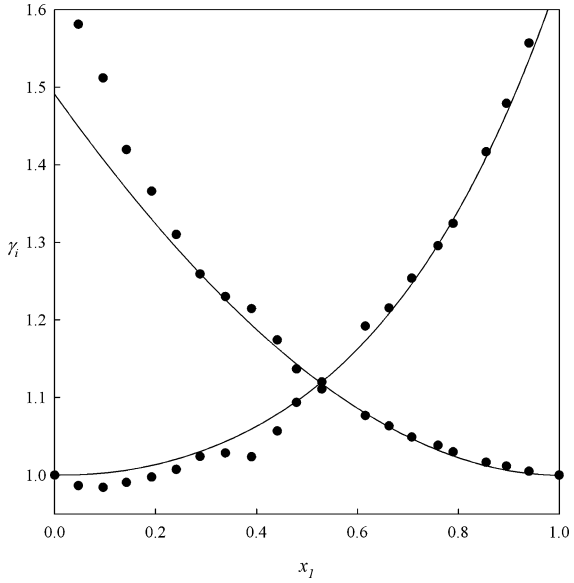

Figure 3. Activity coefficient plot for the system hexane (1) + DMF (2) at 50.00 kPa: ●, experimental data; —, predicted from the two-parameter Legendre polynomial used in consistency analysis (Table 7).

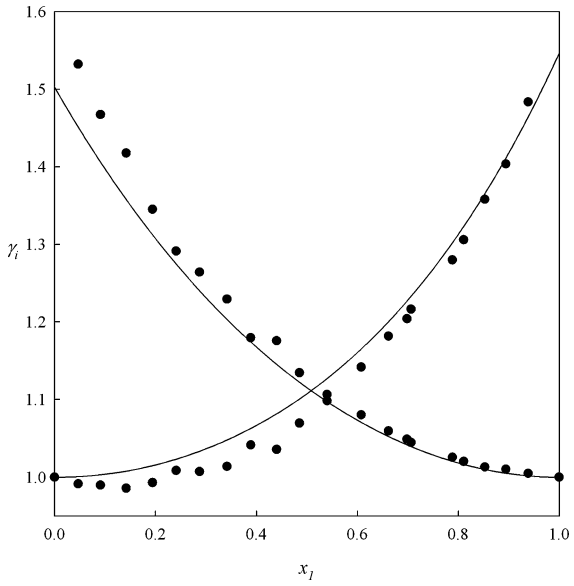

Figure 4. Activity coefficient plot for the system hexane (1) + DMF (2) at 75.00 kPa: ●, experimental data; —, predicted from the two-parameter Legendre polynomial used in consistency analysis (Table 7).

$$\ln \gamma_i = \ln \frac{y_i P}{x_i P_i^0} + \frac{(B_{ii} - V_i^L)(P - P_i^0)}{RT} + y_j^2 \frac{P}{RT}(2B_{ij} - B_{jj} - B_{ii}) \quad (3)$$

In eq 3 R is the universal gas constant, P is the total pressure, P_i^0 is the pure component vapor pressure (see eqs 1 and 2), V_i^L is the liquid molar volume of component i, which was calculated from the Rackett's correlation.[24] B_{ii}, B_{jj}, and B_{ij} are the

dx.doi.org/10.1021/je300631s | J. Chem. Eng. Data 2012, 57, 2681−2688

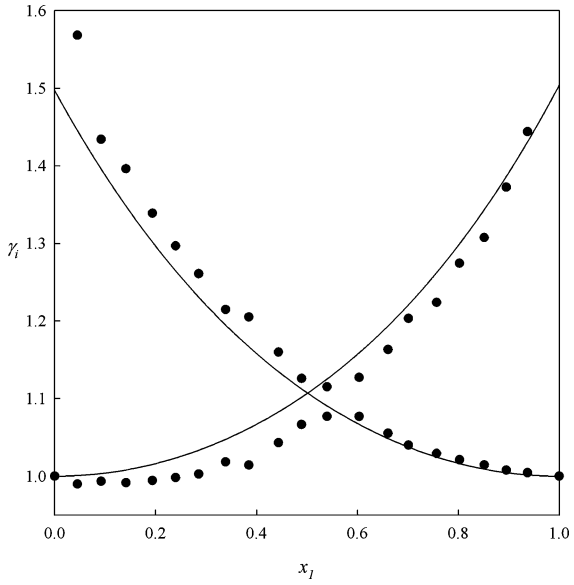

Figure 5. Activity coefficient plot for the system hexane (1) + DMF (2) at 94.00 kPa: ●, experimental data; —, predicted from the two-parameter Legendre polynomial used in consistency analysis (Table 7).

second virial coefficients of the pure gases and the cross value for mixture, respectively. In this work, these coefficients were calculated by using the method of Tsonopoulos[25] and their numerical values are presented in Tables 4 to 6. Considering the point-to-point consistency method proposed by Van Ness et al.[26] and modified later by Fredenslund et al.[27] together with the Barker's[28] reduction method, it is possible to establish that for each isobaric condition $\Delta y < 0.01$, thus implying that the VLE reported in Tables 4 to 6 are thermodynamically consistent. In addition to the point-to-point consistency method, the experimental VLE data have been correlated with a Legendre polynomial. According to statistical analysis,[29] two parameters are adequate to fit the equilibrium vapor pressure at each isobaric condition. Table 7 summarizes the Legrendre polynomial coefficients and their consistency statistics.

To provide reliable and transferable VLE parameters, the VLE data reported in this work have been correlated with classical activity coefficient models, such as Wohl, nonrandom two-liquid (NRTL), Wilson, and universal quasichemical (UNIQUAC).[30] See Walas' textbook for a general discussion of these models.[31] Table 8 summarizes the corresponding parameters together with the relative deviation for the case of bubble and dew point pressures. According to the results presented in Table 8, it is possible to conclude that all the fitted activity coefficient models exhibit a good correlation of the binary system at the three isobaric conditions.

Table 7. Consistency Test Statistics for the Binary System Hexane (1) + DMF (2)

P				δP^c
kPa	$L_1{}^a$	$L_2{}^a$	$100 \times \Delta y^b$	kPa
50.00	0.4482	0.0491	0.5	0.1
75.00	0.4218	0.0146	0.7	0.2
94.00	0.4060	0.0024	0.8	0.2

[a]Parameters for the Legendre polynomial[27] used in consistency. [b]Average absolute deviation in vapor-phase mole fractions $\Delta y = (1/N)\Sigma_{i=1}^{N}|y_i^{exp} - y_i^{cal}|$ (N: number of data points). [c]Average absolute deviation in vapor pressure $\Delta P = (1/N)\Sigma_{i=1}^{N}|P_i^{exp} - P_i^{cal}|$.

Excess Volume Data. The experimental mass densities of the pure components (ρ_i) and of the mixture (ρ) at $T = 298.15$ K and atmospheric pressure are presented in Table 9. Excess volumes (V^E) of the mixture can be calculated from the experimental mass densities according to the equation:

$$V^E = \frac{x_1M_1 + x_2M_2}{\rho} - x_1\frac{M_1}{\rho_1} - x_2\frac{M_2}{\rho_2} \quad (4)$$

In eq 4, M_i is the molecular weight of pure components whose values were taken from ref 21. The V^E results are reported in Table 9 and illustrated in Figure 6. The results presented in the quoted table and figure indicate that the V^E of the hexane (1) + DMF (2) mixture are positive. The V^E results have been smoothed by using the Redlich–Kister expansion:[32]

Table 8. Parameters and Prediction Statistics for Different Gibbs Excess (G^E) Models in Hexane (1) + DMF (2)[a,b]

					bubble-point pressures		dew-point pressures	
	P				ΔP^f		ΔP^f	
model	kPa	A_{12}	A_{21}	α_{12}	%	$100 \times \Delta y_i^g$	%	$100 \times \Delta x_i^g$
Wohl	50.00	0.424	0.505	0.841[e]	0.38	0.4	0.72	0.4
	75.00	0.394	0.462	0.788[e]	0.19	0.6	0.69	0.6
	94.00	0.383	0.441	0.856[e]	0.23	0.7	0.80	0.8
NRTL	50.00	1705.97	−270.50	0.30	0.37	0.5	0.67	0.4
	75.00	1673.56	−301.15	0.30	0.35	0.6	0.78	0.6
	94.00	1640.52	−298.30	0.30	0.43	0.7	0.89	0.8
Wilson[c]	50.00	−426.07	1822.41		0.32	0.5	0.67	0.4
	75.00	−460.00	1782.48		0.22	0.6	0.71	0.7
	94.00	−466.14	1756.60		0.28	0.8	0.82	0.9
UNIQUAC[d]	50.00	918.10	−500.41		0.45	0.5	0.88	0.5
	75.00	1069.10	−632.31		0.18	0.7	0.70	0.7
	94.00	1064.55	−636.00		0.19	0.8	0.83	0.9

[a]The parameters have been calculated by minimizing the objective function: $OF = \Sigma_i^N(|P_i^{exp} - P_i^{cal}|/P_i^{cal} + |y_i^{exp} - y_i^{cal}|)^2$. [b]$A_{12}$ and A_{21} are the G^E model parameters in J·mol^{-1}. [c]Liquid molar volumes have been estimated from the Rackett equation.[24] [d]The molecular parameters r and q are those reported in DECHEMA:[20] $r_1 = 4.4998$, $r_2 = 3.9208$, $q_1 = 3.8560$, $q_2 = 3.0840$. [e]"q" parameter for the Wohl's model. [f]$\Delta P = (100/N)\Sigma_i^N|P_i^{exp} - P_i^{cal}|/P_i^{exp}$. [g]$\Delta\delta = (1/N)\Sigma_i^N|\delta_i^{exp} - \delta_i^{cal}|$ with $\delta = y$ or x.

dx.doi.org/10.1021/je300631s | J. Chem. Eng. Data 2012, 57, 2681–2688

Table 9. Densities ρ and Excess Volumes V^E as a Function of the Liquid Mole Fraction (x_1) for the Binary System Hexane (1) + DMF (2) at Temperature T = 298.15 K and Pressure p = 101.3 kPa[a]

	ρ	$10^3 \cdot V^E$
x_1	g·cm^3	cm^3·mol^{-1}
0.000	0.89570	0
0.058	0.87843	52
0.103	0.86507	108
0.169	0.84648	166
0.211	0.83486	189
0.284	0.81533	241
0.326	0.80435	254
0.373	0.79242	283
0.425	0.77922	322
0.474	0.76735	338
0.523	0.75553	355
0.577	0.74304	348
0.671	0.72212	321
0.730	0.70938	272
0.854	0.68363	182
0.915	0.67156	107
0.979	0.65909	50
1.000	0.65517	0

[a]Standard uncertainties u are $u(x_1)$ = ± 0.01, $u(\rho)$ = 5·10^{-6} g·cm^{-3}, $u(T)$ = ± 0.01 K, $u(p)$ = ± 0.03 kPa.

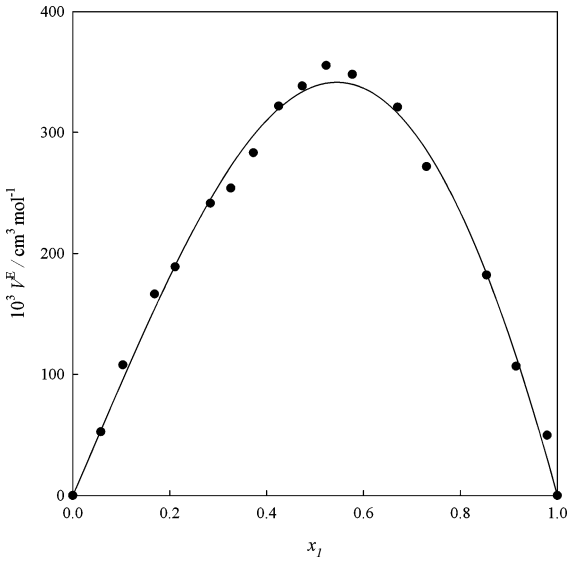

Figure 6. Excess volumes (V^E) as a function of the liquid (x_1) for the system hexane (1) + DMF (2) at 298.15 K and 101.3 kPa: ●, experimental data; —, smoothed by a Redlich–Kister expansion with the parameters reported in Table 10.

$$V^E = x_1 x_2 \sum_{k=0}^{m} c_k (x_2 - x_1)^k \quad (5)$$

In eq 5 m is the number of c_k parameters, which can be found by applying a nonlinear least-squares technique. Table 10 summarizes the c_k parameters together with the correlation statistics.

Interfacial Tension Data. The experimental interfacial tensions of the pure components (σ_i) and of the mixture (σ) at T = 303.15 K and atmospheric pressure are presented in Table 11

Table 10. Coefficients (c_0 and c_1) and Deviations (Maximum (max dev), Average (avg dev), and Standard (st dev)) Obtained in Correlation of Excess Volumes, Eq 5, for the Hexane (1) + DMF (2) at 298.15 K and 101.3 kPa

c_0	c_1	c_2	max dev	avg dev	st dev
cm^3·mol^{-1}	cm^3·mol^{-1}	cm^3·mol^{-1}	10^3 cm^3·mol^{-1}	10^3 cm^3·mol^{-1}	10^3 cm^3·mol^{-1}
1.35338	−0.27680	−0.16048	0.365	0.099	0.118

Table 11. Interfacial Tensions σ as a Function of the Liquid Mole Fraction x_1 for the Binary System Hexane (1) + DMF (2) at Temperature T = 303.15 K and Pressure p = 101.3 kPa[a]

	σ
x_1	mN·m^{-1}
0.000	23.60
0.048	22.32
0.095	21.63
0.189	20.75
0.295	20.12
0.397	19.36
0.502	19.14
0.606	18.70
0.723	18.40
0.811	18.15
0.915	17.82
0.970	17.49
1.000	17.40

[a]Standard uncertainties u are $u(x_1)$ = ± 0.01, $u(\sigma)$ = ± 0.2 mN·m^{-1}, $u(T)$ = ± 0.01 K, $u(p)$ = ± 0.03 kPa.

and depicted in Figure 7. From the indicated figure it is possible to observe that σ exhibits lower values than $x_1\sigma_1 + x_2\sigma_2$ in the whole

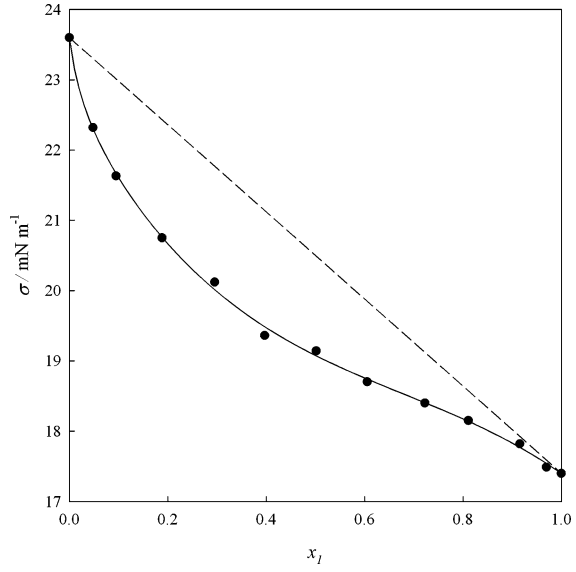

Figure 7. Interfacial tension (σ) as a function of the liquid mole fraction (x_1) for the system hexane (1) + DMF (2) at 303.15 K and 101.3 kPa: ●, experimental data; - - -, linear behavior ($x_1\sigma_1 + x_2\sigma_2$); —, smoothed with a Myers–Scott expansion using the parameters reported in Table 12.

mole fraction range, thus presenting a negative deviation from the linear behavior. The IFT data were correlated using the Myers–Scott (MS) expansion:[33]

dx.doi.org/10.1021/je300631s | J. Chem. Eng. Data 2012, 57, 2681–2688

$$\sigma = \frac{x_1 x_2}{1 - b(1 - 2x_1)} \sum_{k=0}^{m} c_k (x_2 - x_1)^k + (x_1\sigma_1 + x_2\sigma_2) \quad (6)$$

In eq 6 m and c_k have the same meaning as in eq 5, and b is an extra parameter. Equation 6 reduces to the Redlich−Kister expansion when $b = 0$, and cases for $b \neq 0$ yield more smoothing flexibility. The parameters c_k and b together with the correlation statistics are reported in Table 12.

Table 12. Coefficients (c_0, c_1, and c_2) and Deviations (Maximum (max dev), Average (avg dev), and Standard (st dev)) Obtained in Correlation of Interfacial Tension, Eq 6, for the Hexane (1) + DMF (2) at 303.15 K and 101.3 kPa

c_0	c_1	c_2		max dev	avg dev	st dev
$mN{\cdot}m^{-1}$	$mN{\cdot}m^{-1}$	$mN{\cdot}m^{-1}$	B	10^3 $mN{\cdot}m^{-1}$	10^3 $mN{\cdot}m^{-1}$	10^3 $mN{\cdot}m^{-1}$
−5.6921	$9.49{\cdot}10^{-5}$	3.1203	0.9467	6.56	2.06	2.10

CONCLUSIONS

Subcritical isobaric vapor−liquid equilibrium (VLE) data at (50, 75, and 94) kPa, atmospheric mixing volumes at 298.15 K, and interfacial tensions at 303.15 K have been measured for the hexane + DMF binary mixture. Experimental VLE data show that hexane + DMF binary mixture positively deviates from the Raoult's behavior. Excess volumes exhibit positive deviation, showing a maximum of 0.3554 $cm^3{\cdot}mol^{-1}$ at $x_1 = 0.523$. The interfacial tensions, in turn, exhibit negative deviation from the linear behavior.

Traditional activity coefficient models, such as Wohl, NRTL, Wilson, and UNIQUAC, are capable of correlating the activity coefficients and boiling points with the mole fraction. According to the results, the best activity coefficients fit corresponds to the Wohl model. The excess volumes and interfacial tensions of the hexane + DMF binary mixture were smoothed and well represented by the Redlich−Kister and Myers−Scott equations, respectively.

AUTHOR INFORMATION

Corresponding Author

*E-mail: A.M., amejia@udec.cl; H.S., hsegura@udec.cl.

Funding

This work was financed by FONDECYT, Santiago, Chile (Project 1120228).

Notes

The authors declare no competing financial interest.

REFERENCES

(1) Directive 2009/28/EC of the European Parliament ad of the Council on the promotion of the use of energy from renewable sources.

(2) Román-Leshkov, Y.; Barrett, C. J.; Liu, Z. Y.; Dumesic, J. A. Production of dimethylfuran for liquid fuels from biomass-derived carbohydrates. *Nature* **2007**, *447*, 982−985.

(3) Binder, J. B.; Raines, R. T. Simple chemical transformation of lignocellulosic biomass into furans for fuels and chemicals. *J. Am. Chem. Soc.* **2009**, *131*, 1979−1985.

(4) Nakata, K.; Uchida, D.; Ota, A.; Utsumi, S.; Kawatake, K. The impact of RON on SI engine thermal efficiency. *SAE* **2007**, 01−2007.

(5) Zhong, S.; Daniel, R.; Xu, H.; Zhang, J.; Turner, D.; Wyszynski, M. L.; Richards, P. Combustion and Emissions of 2,5-Dimethylfuran in a Direct-Injection Spark-Ignition Engine. *Energy Fuels* **2010**, *24*, 2891−2899.

(6) Dumesic, J. A.; Roman-Leshkov, Y.; Chheda, J. N. Catalytic process for producing furan derivatives from carbohydrates in a biphasic reactor. Canada Patent CA 2653706, 2007.

(7) Wu, X.; Huang, Z.; Yuan, T.; Zhang, K.; Wei, L. Identification of combustion intermediates in a low-pressure premixed laminar 2,5-dimethylfuran/oxygen/argon flame with tunable synchrotron photoionization. *Combust. Flame* **2009**, *156*, 1365−1376.

(8) Daniel, R.; Tian, G.; Xu, H.; Wyszynski, M. L.; Wu, X.; Huang, Z. Effect of spark timing and load on a DISI engine fuelled with 2,5-dimethylfuran. *Fuel* **2011**, *90*, 449−458.

(9) Verevkin, S. P.; Welle, F. M. Thermochemical Studies for Determination of the Standard Molar Enthalpies of Formation of Alkyl- Substituted Furans and Some Ethers. *Struct. Chem.* **1998**, *9*, 215−221.

(10) Auwers, K. V. Spectrochemical studies. *Justus Liebigs Ann. Chem.* **1915**, *408*, 212−284.

(11) Daubert, T. E.; Danner, R. P. *Physical and Thermodynamic Properties of Pure Chemicals. Data Compilation*; Taylor and Francis: Bristol, PA, 1989.

(12) Aldrich, http://www.sigmaaldrich.com (retrieved August, 2012).

(13) Alvarez, R.; Medina, I.; Bueno, J. L.; Coca, J. Binary Gaseous Diffusion Coefficients. Air With Methylfuran Derivatives. *J. Chem. Eng. Data* **1983**, *28*, 155−156.

(14) Weir, R. D. D.; de Loos T. W. W. *Measurement of the Thermodynamic Properties of Multiple Phases*; Elsevier: Amsterdam, 2006; Vol. *VII*.

(15) Mejía, A.; Segura, H.; Cartes, M. Vapor−Liquid Equilibria and Interfacial Tensions of the System Ethanol + 2-Methoxy-2-methylpropane. *J. Chem. Eng. Data* **2010**, *55*, 428−434.

(16) Mejía, A.; Cartes, M.; Segura, H. Interfacial tensions of binary mixtures of ethanol with octane, decane, dodecane and tetradecane. *J. Chem. Thermodyn.* **2011**, *43*, 1395−1400.

(17) Mejía, A.; Segura, H.; Cartes, M. Vapor−liquid equilibria and interfacial tensions of the system ethanol + 2-methoxy-2-methylbutane. *J. Chem. Eng. Data* **2011**, *56*, 3142−3148.

(18) Mejía, A.; Segura, H.; Cartes, M. Measurement and theoretical prediction of the vapor−liquid equilibrium, densities and interfacial tensions of the system hexane + 2-methoxy-2-methylbutane. *Fluid Phase Equilib.* **2011**, *308*, 15−24.

(19) Mejía, A.; Segura, H.; Cartes, M.; Pérez-Correa, J. R. Experimental determination and theoretical modeling of the vapor−liquid equilibrium and surface tensions of hexane + tetrahydro-2H-pyran. *Fluid Phase Equilib.* **2012**, *316*, 55−65.

(20) DECHEMA Gesellschaft für Chemische Technik und Biotechnologie e.V., Frankfurt am Main, Germany, https://cdsdt.dl.ac.uk/detherm/ (retrieved August, 2012).

(21) Lemmon, E. W.; McLinden, M. O.; Friend, D. G. Thermophysical Properties of Fluid Systems. In *NIST Chemistry WebBook*; NIST Standard Reference Database Number 69; Linstrom, P. J., Mallard, W. G., Eds.; National Institute of Standards and Technology: Gaithersburg MD; http://webbook.nist.gov (retrieved August, 2012).

(22) Zaitri, L. K.; Negadi, L.; Mokbel, I.; Msakni, N.; Jose, J. Liquid−vapor equilibria of binary systems containing alcohols (1-butanol, or 2-butanol or 1-hexanol) present in the production by chemical process of 2,5-dimethyl furan from biomass. *Fuel* **2012**, *95*, 438−445.

(23) Van Ness, H. C.; Abbott, M. M. *Classical Thermodynamics of Nonelectrolyte Solutions*; McGraw-Hill Book Co.: New York, 1982.

(24) Rackett, H. G. Equation of state for saturated liquids. *J. Chem. Eng. Data* **1970**, *15*, 514−517.

(25) Tsonopoulos, C. An empirical correlation of second virial coefficient. *AIChE J.* **1974**, *20*, 263−272.

(26) Van Ness, H. C.; Byer, S. M.; Gibbs, R. E. Vapor - liquid equilibrium: Part I. An appraisal of data reduction methods. *AIChE J* **1973**, *19*, 238−244.

(27) Fredenslund, Aa.; Gmehling, J.; Rasmussen, P. *Vapor-Liquid Equilibria Using UNIFAC, A Group Contribution Method*. Elsevier: Amsterdam, 1977.

(28) Barker, J. A. Determination of Activity Coefficients from total pressure measurements. *Aust. J. Chem.* **1953**, *6*, 207−210.
(29) Wisniak, J.; Apelblat, A.; Segura, H. An Assessment of Thermodynamic Consistency Tests for Vapor-Liquid Equilibrium Data. *Phys. Chem Liq.* **1997**, *35*, 1−58.
(30) Prausnitz, J. M.; Lichtenthaler, R. N.; Gomes de Azevedo, E. *Molecular Thermodynamics of Fluid-Phase Equilibria*, 3th ed.; Prentice-Hall: Englewood Cliffs, NJ, 1999.
(31) Walas, S. M. *Phase Equilibria in Chemical Engineering*, Butterworth-Heinemann: London, 1985.
(32) Redlich, O; Kister, A. T. Thermodynamics of nonelectrolyte solutions - x-y-t relations in a binary system. *Ind. Eng. Chem.* **1948**, *40*, 341−345.
(33) Myers, D. B.; Scott., R. L. Thermodynamic functions for nonelectrolyte solutions. *Ind. Eng. Chem.* **1963**, *55*, 43−46.